Article

Theory Favors a Stepwise Mechanism of Porphyrin Degradation by a Ferric Hydroperoxide Model of the Active Species of Heme Oxygenase

Devesh Kumar, Samul P. de Visser, and Sason Shaik

J. Am. Chem. Soc., **2005**, 127 (22), 8204-8213• DOI: 10.1021/ja0446956 • Publication Date (Web): 12 May 2005

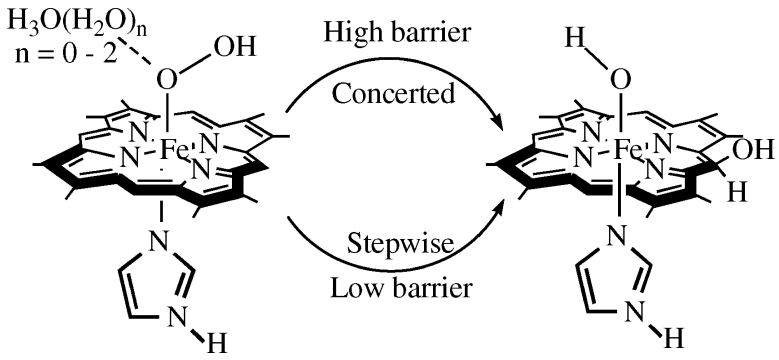

More About This Article

Additional resources and features associated with this article are available within the HTML version:

- Supporting Information
- Links to the 9 articles that cite this article, as of the time of this article download
- Access to high resolution figures
- Links to articles and content related to this article
- Copyright permission to reproduce figures and/or text from this article

View the Full Text HTML

J|A|C|S
ARTICLES
Published on Web 05/12/2005

Theory Favors a Stepwise Mechanism of Porphyrin Degradation by a Ferric Hydroperoxide Model of the Active Species of Heme Oxygenase

Devesh Kumar, Samuël P. de Visser, and Sason Shaik*

Contribution from the Department of Organic Chemistry and the Lise Meitner-Minerva Center for Computational Quantum Chemistry, The Hebrew University, Jerusalem 91904, Israel

Received September 2, 2004; E-mail: sason@yfaat.ch.huji.ac.il

Abstract: The report uses density functional theory to address the mechanism of heme degradation by the enzyme heme oxygenase (HO) using a model ferric hydroperoxide complex. HO is known to trap heme molecules and degrade them to maintain iron homeostasis in the biosystem (Ortiz de Montellano, P. R. *Acc. Chem. Res.* **1998**, *31*, 543). The degradation is initiated by complexation of the heme, then formation of the iron−hydroperoxo species, which subsequently oxidizes the *meso* position of the porphyrin by hydroxylation, thereby enabling eventually the cleavage of the porphyrin ring. Kinetic isotope effect studies (Davydov, R.; Matsui, T.; Fujii, H.; Ikeda-Saito, M.; Hoffman, B. M. *J. Am. Chem. Soc.* **2003**, *125*, 16208) indicate that the mechanism is assisted by general acid catalysis, via a chain of water molecules, and that all the events occur in concert. However, previous theoretical treatments indicated that the concerted mechanism has a high barrier, much higher than an alternative mechanism that is initiated by O−O bond homolysis of iron−hydroperoxide (Sharma, P. K.; Kevorkiants, R.; de Visser, S. P.; Kumar, D.; Shaik, S. *Angew. Chem. Int. Ed.* **2004**, *43*, 1129). The present contribution studies the stepwise and concerted acid-catalyzed mechanisms using $H_3O^+(H_2O)_n$, $n = 0-2$. The effect of the acid strength is tested using the $H_4N^+(H_2O)_2$ cluster and a fully protonated ferric hydroperoxide. All the calculations show that *a stepwise mechanism that involves proton relay and O−O homolysis, in the rate-determining step, has a much lower barrier (>10 kcal/mol) than the corresponding fully concerted mechanism.* The best fit of the calculated solvent kinetic isotope effect, to the experimental data, is obtained for the $H_3O^+(H_2O)_2$ cluster. The calculated α-deuterium secondary kinetic isotope effect is inverse (0.95−0.98), but much less so than the experimental value (0.7). Possible reasons for this quantitative difference are discussed. Some probes are suggested that may enable experiment to distinguish the stepwise from the concerted mechanism.

Introduction

The enzyme heme oxygenase (HO) traps iron porphyrin (heme, **1** in Scheme 1a) molecules and leads to their degradation, to maintain iron homeostasis and other important biofunctions.[1,2] According to structural studies,[2a] the trapped heme is axially coordinated through the iron atom by an imidazole ring of a histidine residue and a water molecule, Scheme 1a. Upon dioxygen uptake followed by two-electron reduction and protonation, a ferric hydroperoxide complex, Fe−OOH (**2**, in Scheme 1) is formed, which eventually causes hydroxylation at the α-*meso* position of the porphyrin. Subsequently, the *meso*-hydroxylated species (α-*meso*-hydroxyheme, Scheme 1a) undergoes oxidative ring opening and releases iron and carbon monoxide.

Initial mechanistic investigations[1a,3−5a] established that the active species of the enzyme is the ferric hydroperoxide (**2**, Scheme 1a), and that the competent reaction intermediate leading

(1) (a) Ortiz de Montellano, P. R. *Acc. Chem. Res.* **1998**, *31*, 543. (b) Ortiz de Montellano, P. R. *Curr. Opin. Chem. Biol.* **2000**, *4*, 221. (c) Colas, C.; Ortiz de Montellano, P. R. *Chem. Rev.* **2003**, *103*, 2305. (d) Yoshida, T.; Migita, C. T. *J. Inorg. Biochem.* **2000**, *82*, 33. (e) Sono, M.; Roach, M. P.; Coulter, E. D.; Dawson, J. H. *Chem. Rev.* **1996**, *96*, 2841.

(2) (a) Schuller, D. J.; Wilks, A.; Ortiz de Montellano, P. R.; Poulos, T. L. *Nature Struct. Biol.* **1999**, *6*, 860. (b) Lad, L.; Friedman, J.; Li, H.; Ortiz de Montellano, P. R.; Poulos, T. *Biochemistry*, **2004**, *43*, 3793. (c) Lightning, L. K.; Huang, W.-w.; Moenne-Loccoz, P.; Loehrs, T. M.; Schuller, D. J.; Poulos, T. L.; Ortiz de Montellano, P. R. *J. Biol. Chem.* **2001**, *276*, 10612. (d) Lad, L.; Wang, J.; Li, H.; Friedman, J.; Bhashkar, B.; Ortiz de Montellano, P. R.; Poulos, T. *J. Mol. Biol.* **2003**, *330*, 527. (e) Friedman, J.; Lad, L.; Deshmukh, R.; Li, H.; Wilks, A.; Poulos, T. L. *J. Biol. Chem.* **2003**, *278*, 34654. (f) Fuji, H.; Zhang, X.; Tomita, T.; Ikeda-Saito, M.; Yoshida, T. *J. Am. Chem. Soc.* **2001**, *123*, 6475. (g) Unno, M.; Matsui, T.; Chu, G. C.; Couture, M.; Yoshida, T.; Rousseau, D. L.; Olson, J. S.; Ikeda-Saito, M. *J. Biol. Chem.* **2004**, *279*, 21055. (h) Hirotu, S.; Chu, G. C.; Unno, M.; Lee, D.-S.; Yoshida, T.; Park, S.-M.; Shiro, Y.; Ikeda-Saito, M. *J. Biol. Chem.* **2004**, *279*, 11937.

(3) (a) Wilks, A.; Torpey, J.; Ortiz de Montellano, P. R. *J. Biol. Chem.* **1994**, *269*, 29553. (b) Liu, Y.; Ortiz de Montellano, P. R. *J. Biol. Chem.* **2000**, *275*, 5297.

(4) Coupled oxidation studies of histidine enzymes such as myoglobin, and cyt_{b5} as well as specific mutants of these enzymes were shown to induce α-*meso* hydroxylation via the ferric hydroperxide species, see e.g., (a) Murukami, T.; Morishima, I.; Toshikata, M.; Ozaki, S.-i.; Hara, I.; Yang, H.-J.; Watanabe, Y. *J. Am. Chem. Soc.* **1999**, *121*, 2007; Avila, L.; Huang, H.-w.; Rodriguez, J. C.; Möenne-Loccoz, P.; Rivera, M. *J. Am. Chem. Soc.* **2000**, *122*, 7618; Avila, L.; Huang, H.-w.; Damaso, C. O.; Lu, S.; Möenne-Loccoz, P.; Rivera, M. *J. Am. Chem. Soc.* **2003**, *125*, 4103. These, and mutation studies of HO (ref 2) that convert the enzyme to a peroxidase, show that the acid functionality and hydrogen bond network is necessary for HO. *However, since other heme enzymes can be made to mimic HO activity, there is nothing particularly special about HO itself.* (b) Note that coupled oxidation mechanism may involve in some cases a component of direct oxidation by uncoordinated H_2O_2, which is not the mechanism investigated in the present paper. See for example, ref 4a and, St Claire, T. N.; Balch, A. L. *Inorg. Chem.* **1999**, *38*, 684.

10.1021/ja0446956 CCC: $30.25

Scheme 1. (a) Degradation of Heme by Heme Oxygenase (HO);[a] (b) Experimental[5b] Kinetic Isotope Effect Values and the Proposed Proton-Catalyzed Concerted Mechanism

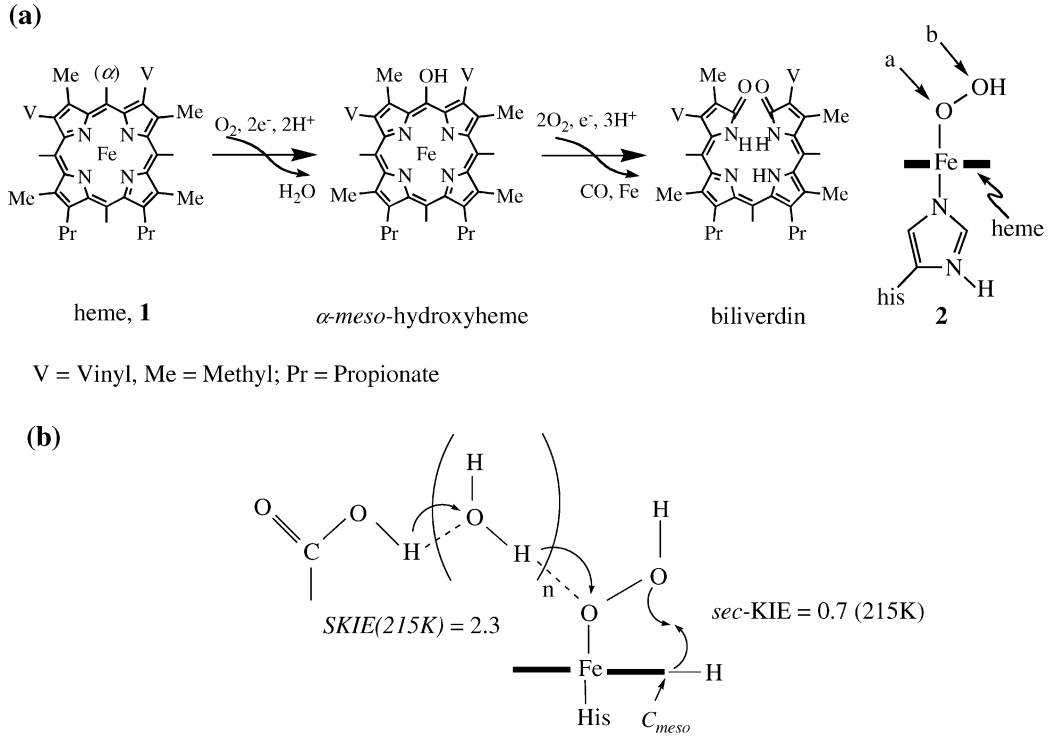

[a] Active species is **2**.[1a,3,5a]

to biliverdin is the α-*meso*-hydroxyheme species (in Scheme 1a). On the basis of the experimental data it was suggested that the process involves a concerted electrophilic hydroxylation by **2**.[1a,b,3] A subsequent EPR/ENDOR study by Davydov et al.[5b] measured solvent kinetic isotope effect (SKIE) and secondary α-deuterium kinetic isotope effect (*sec*-KIE) at the *meso*-carbon position of the porphyrin and provided evidence for a fully concerted mechanism that is summarized in Scheme 1b along with the isotope effect values. According to a classical interpretation,[6a,b] the inverse *sec*-KIE(H_{meso}/D_{meso}) of 0.7 (at 215 K) indicates that at the transition state, the *meso* carbon begins to undergo rehybridization from sp^2 to sp^3. In turn, according to the semiclassical theory of solvent isotope effect,[6c] the SKIE-(H_2O/D_2O) value of 2.3 signifies that water molecules relay a proton to the ferric hydroperxo in synchronicity with the O−O cleavage and the attack on the *meso*-carbon position.

However, theoretical density functional studies by two different groups[7] found the concerted mechanism, starting from a model complex of **2**, to be *of very high energy*. One of the studies[7a] showed that a stepwise mechanism which involves O−O bond homolysis in the first step has a much lower barrier compared with that of the concerted alternative. It was further demonstrated[7a] that the O−O bond homolysis step can be catalyzed by proton transfer from water molecules to give the ferric hydrogen peroxide complex, $Fe(H_2O_2)^+$, which undergoes a more facile O−O homolyis compared with bare Fe−OOH. With or without protonation, the calculated barriers for the stepwise heme-hydroxylation mechanisms were much lower than the corresponding concerted mechanisms.[7a] The new experimental conclusion[5b] and the importance of the HO mechanism prompted us to undertake a detailed study of concerted and stepwise *meso*-hydroxylation mechanisms of a model of **2**, activated by proton transfer from a protonated cluster of water molecules, $H_3O^+(H_2O)_n$, $n = 0-2$. As a test of the acid strength effect, we looked at $NH_4^+(H_2O)_2$ where the water cluster is coordinated to a weaker acid. In addition, it was deemed necessary to characterize the SKIE(D_2O/H_2O) and *sec*-KIE-(H_{meso}/D_{meso}) values of the concerted vis-à-vis the stepwise mechanisms of *meso*-hydroxylation, and to determine some new KIE probes that may serve to distinguish the two mechanisms. Such characterization will provide *the intrinsic features* of the reactive species without the involvement of the constraints in the protein pocket[4] and may thereby test the ability of KIE measurements to probe the structure of the transition state. At the same time the results may shed light on the origins of the apparent disparity between theory and experiment and suggest some new experimental probes, hence promoting a fruitful dialogue between experiment and theory.

Systems and Methods

System. Scheme 2 shows the model system that was used to probe the mechanisms and corresponding KIE features. The system involves a ferric hydroperoxide heme species, **2**, where the histidine is replaced by an imidazole (ImH) ligand and the heme by iron porphine. Thus, our model species corresponds to the proposed active species of HO where the OOH group is coordinated to the iron, not as in the coupled

(5) (a) Davydov, R.; Kofman, V.; Fujii, H.; Yoshida, T.; Ikeda-Saito, M.; Hoffman, B. M. *J. Am. Chem. Soc.* **2002**, *124*, 1798. (b) Davydov, R.; Matsui, T.; Fujii, H.; lkeda-Saito, M.; Hoffman, B. M. *J. Am. Chem. Soc.* **2003**, *125*, 16208.

(6) (a) Melander, L.; Saunders, W. H., Jr. In *Reaction rates of isotopic molecules*.; Robert E. Krieger Publishing Company: Malabar, Florida, 1987; pages 172−174. (b) Streitwieser, A., Jr.; Jagow, R. H.; Fahey, R. C.; Suzuki, S. *J. Am. Chem. Soc.* **1958**, *80*, 2326. (c) Schowen, R. L. In *Isotope Effects on Enzyme-Catalyzed Reactions*; Cleland, W. W., O'Leary, M. H., Northrop, D. B., Eds.; University Park Press: Baltimore, 1977; pages 64−100.

(7) (a) Sharma, P. K.; Kevorkiants, R.; de Visser, S. P.; Kumar, D.; Shaik, S. *Angew. Chem., Int. Ed.* **2004**, *43*, 1129. (b) Kamachi, T.; Shestakov, A. F.; Yoshizawa, K. *J. Am. Chem. Soc.* **2004**, *126*, 3672.

Scheme 2. Model Systems Used in the Study

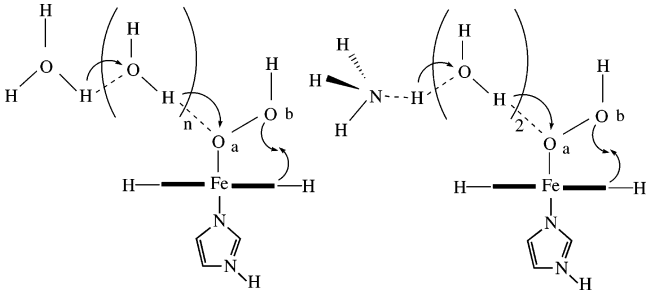

oxidation process where some of the *meso* oxidation is proposed to be mediated by noncoordinated hydrogen peroxide.[4b] Furthermore, mutation studies of other enzymes (Mb, Cyt$_{b5}$) lead to mutants with HO activity,[4a] while mutations of the acid functionality of HO, e.g., Asp$_{140}$ in human HO-1, disrupts HO activity and converts the enzyme to a peroxidase.[2c,d] *This means that while the acid functionality of HO is essential for HO activity, other features are less critical since other enzymes can be made to act as HO.*[4a] This, in turn, suggests that a minimal realistic system, which is appropriate for studying the mechanistic choice, must involve the ferric hydroperoxide species and a proton relay machinery, as in Scheme 2.

Following the experimental findings,[2c−h,8] of a network of waters that hydrogen bond to the distal ligand, we computed the process in the presence of an acid coordinated to a cluster of water molecules where we varied the number of coordinated water molecules from n = 0 to 2. On the basis of experimental criteria, the postulated acids vary with the enzyme: e.g., a neutral carboxylic acid residue,[5b] an aspartate-arginine ion-pair,[2f] or a water molecule coordinated to an arginine side chain.[2e] In our study, we had to use a protonated cluster of water molecules. This avoids the ion-pair situation as a starting model or as the product species that would have been generated by use of a neutral acid. Such ion-pair situations are not properly handled by the gas-phase computations employed here. Thus, our proton source is a more potent catalyst than the carboxylic acid−water cluster (or carboxylate−arginine−water) that is presumed to catalyze the process.[5b] Therefore, to test the dependence of the conclusions on the acid strength, we also examined the reaction with a cluster of water coordinated to an ammonium cation, $NH_4^+(H_2O)_2$ in Scheme 2. Note that in both modes in Scheme 2, the acid also polarizes the water molecules and enables them to participate in proton relay to the active center. As such, the present models, together with the previously studied ones[7a] using an unprotonated pristine **2** and a fully protonated complex *form a range of acidity that includes the strength of a neutral acid as suggested in the real enzyme*.

For each $H_3O^+(H_2O)_n$ cluster, we studied both the stepwise and concerted mechanisms of *meso*-hydroxylation. To mimic the constraints in the protein pocket,[9] we initially fixed the O_a- - -O_{last} distance between the O_a position of the FeOOH moiety and the oxygen of the last water molecule in the cluster, while letting all other parameters be freely optimized. In this manner the "acid" molecule is fixed in space, in line with the structural information.[2b,c,e] Subsequently, we fully relaxed the O_a- - -O_{last} distance constraint and restrained only the dihedral angles involving the oxygen atoms, which maintain a plane, so as to prevent the collapse of the water network. The following dihedral angles were restrained: in the case of H_3O^+ it is the $O_1-O_a-Fe-N_{por}$ angle, in case of $H_3O^+(H_2O)$ the $O_2-O_1-O_a-O_b$ angle, and in case of $H_3O^+(H_2O)_2$ the angle $O_3-O_2-O_a-O_b$. Release of the distance constraints lead to minor structural changes (See Figures S.1−S.6 in the Supporting Information). These small changes show that the water network is a remarkably robust structure that is determined by H-bonding distances. All the more, the small structural changes were attended by insignificant changes of ≤0.1 kcal/mol in the relative energy of the transition states for the two mechanisms. In the case of $H_4N^+(H_2O)_2$, the dihedrals $N-O_2-O_a-O_b$, $O_2-O_1-O_a-O_b$ were restrained, and the two mechanisms were subsequently scanned and optimized.

Strategy. As found in an earlier study,[7a] the free optimization of the $H_3O^+(H_2O)_2$ system in Scheme 2 resulted always in the initial protonation of the proximal oxygen (O_a) of the FeOO moiety. Therefore, to generate a process where the protonation is concurrent with either O−O bond cleavage or with both O−O cleavage and attack on the *meso* position, we first constrained the proton to the water cluster and optimized a complex between **2** and the $H_3O^+(H_2O)_n$ cluster (the proton moves first through the water chain). Subsequently, we scanned the reaction pathways for concerted and stepwise hydroxylation mechanisms. The concerted mechanism was obtained by tracing a scan along the coordinate that involves the O_b-C_{meso} bond making, while freely optimizing all other parameters. The structure at the top of the scan was subjected then to full geometry optimization and frequency calculation. In the alternative stepwise mechanism, we started from the same optimized cluster, composed of **2** and $H_3O^+(H_2O)_n$, and then followed a scan along the O_a-O_b coordinate leading to cleavage of this bond and to generation of an intermediate species. Subsequently, we ran a scan for the formation of the O_b-C_{meso} bond, while letting all other parameters be freely optimized. The top structures of these scans were then subjected to transition state search and frequency calculations. The same procedure was applied to the ammonium-di-water cluster. Finally, to ascertain the preferred mechanism, we recalculated the energies of the respective transition states in a dielectric medium with a dielectric constant of ϵ = 5.7 and also tested the sensitivity of the results to the conformation of the imidazole, which in the crystal structure[2g] is found to be perpendicular to the plane of the Fe−OO moiety.

Methods. Following established procedures,[7a,10] we used unrestricted hybrid density functional UB3LYP calculations.[11] Since the previous results[7a] with the double-ζ LACVP(Fe)/6-31G(rest)[12,13] and the LACVP**(Fe)/6-31G**(rest) basis sets were virtually identical in all their mechanistic conclusions, we used here the former basis set (hereafter, LACVP). The geometry optimizations were carried out by the JAGUAR 4.5 package,[14] while the frequency and KIE calculations were done with GAUSSIAN-03 package.[15] Due to the constraints imposed on the structures, all of them involved small imaginary frequencies due to rotational modes of the water molecules. We emphasize that invariably, in all cases, the "transition structures" for the concerted process are not true transition states; these species were found to be second-order saddle points that possess an additional imaginary frequency corresponding to the mode that converts the

(8) (a) Li, Y.; Syvitski, R. T.; Auclair, K.; Wilks, A.; Ortiz de Montellano, P. R.; La Mar, G. N. *J. Biol. Chem.* **2002**, *277*, 33018. (b) Syvitski, R. T.; Li, Y.; Auclair, K.; Wilks, A.; Ortiz de Montellano, P. R.; La Mar, G. N. *J. Am. Chem. Soc.* **2002**, *124*, 14296.
(9) Harris, D. L. *J. Inorg. Biochem.* **2002**, *91*, 568.
(10) Ogliaro, F.; de Visser, S. P.; Cohen, S.; Sharma, P. K.; Shaik, S. *J. Am. Chem. Soc.* **2002**, *124*, 2806.
(11) (a) Becke, A. D. *J. Chem. Phys.* **1992**, *96*, 2155−2160. (b) Becke, A. D. *J. Chem. Phys.* **1992**, *97*, 9173−9177. (c) Becke, A. D. *J. Chem. Phys.* **1993**, *98*, 5648−5652. (d) Lee, C.; Yang, W.; Parr, R. G. *Phys. Rev. B* **1988**, *37*, 785−789.
(12) (a) Hay, J. P.; Wadt, W. R. *J. Chem. Phys.* **1985**, *82*, 299−308. (b) Friesner, R. A.; Murphy, R. B.; Beachy, M. D.; Ringlanda, M. N.; Pollard, W. T.; Dunietz, B. D.; Cao, Y. X. *J. Phys. Chem. A* **1999**, *103*, 1913−1928.
(13) Hehre, W. J.; Ditchfield, R.; Pople, J. A. *J. Chem. Phys.* **1972**, *56*, 2257−2261.
(14) *Jaguar 4.2*; Schrödinger, Inc.: Portland, OR, **2000**.
(15) Frisch, M. J.; Trucks, G. W.; Schlegel, H. B.; Scuseria, G. E.; Robb, M. A.; Cheeseman, J. R.; Zakrzewski, V. G.; Montgomery, J. A., Jr.; Stratmann, R. E.; Burant, J. C.; Dapprich, S.; Millam, J. M.; Daniels, A. D.; Kudin, K. N.; Strain, M. C.; Farkas, O.; Tomasi, J.; Barone, V.; Cossi, M.; Cammi, R.; Mennucci, B.; Pomelli, C.; Adamo, C.; Clifford, S.; Ochterski, J.; Petersson, G. A.; Ayala, P. Y.; Cui, Q.; Morokuma, K.; Malick, D. K.; Rabuck, A. D.; Raghavachari, K.; Foresman, J. B.; Cioslowski, J.; Ortiz, J. V.; Baboul, A. G.; Stefanov, B. B.; Liu, G.; Liashenko, A.; Piskorz, P.; Komaromi, I.; Gomperts, R.; Martin, R. L.; Fox, D. J.; Keith, T.; Al-Laham, M. A.; Peng, C. Y.; Nanayakkara, A.; Gonzalez, C.; Challacombe, M.; Gill, P. M. W.; Johnson, B. G.; Chen, W.; Wong, M. W.; Andres, J. L.; Head-Gordon, M.; Replogle, E. S.; Pople, J. A., Gaussian, Inc.: Pittsburgh, PA, 1998.

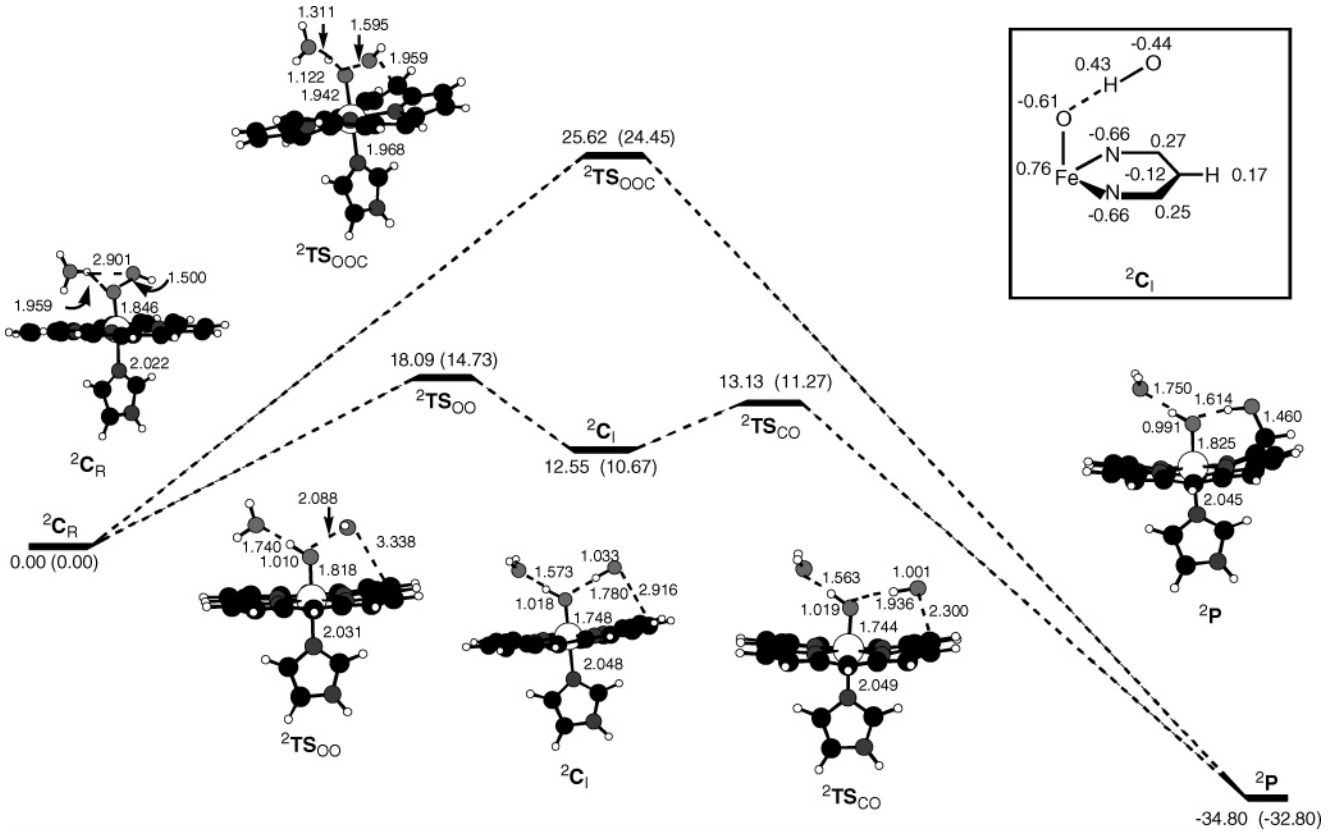

Figure 1. Concerted and stepwise energy profiles for hydroxylation of the *meso* position of porphine by the iron−hydroperoxo species, **2**, of heme oxygenase. The proton source is the hydronium ion. The energies are reported, relative to $^2\mathbf{C}_R$, and the value inside the parentheses include zero-point energy corrections. The drawing inside the box shows the Coulombic cage trapping of the OH• radical species in the stepwise mechanism.

concerted TS to the corresponding stepwise TS. Energy and KIE calculations were done after removal of the imaginary frequencies. To give a measure of the barriers, all energies are referred to the constrained cluster **2**/acid$(H_2O)_n$, labeled later as $^2\mathbf{C}_R$ in Figures 1−4.

Kinetic Isotope Effect Calculations. Kinetic isotope effects (KIEs) were calculated relative to the separated reactants, **2** plus $H_3O^+(H_2O)_n$. As done before,[16] the KIEs were computed from the frequency calculations, after removal of all the imaginary frequencies, by use of the Eyring equation:

$$k_H/k_D = \exp[(\Delta G^{\ddagger}_D - \Delta G^{\ddagger}_H)/RT] \quad (1)$$

where G refers to free energy, R is the gas constant, and T is the temperature. Tunneling corrections were estimated by applying the Wigner correction, again as done before.[16]

Spin States. Since the previous study showed that the dominant state during the first hydroxylation process is the doublet spin-state, we studied only doublet species throughout.

The Effect of Polarity. To mimic a polar environment, we used the solvation model implemented in JAGUAR, using a dielectric constant, $\epsilon = 5.7$, and a probe radius, 2.7 Å, as done in previous studies.[16]

Results and Discussion

Figure 1 displays the two located mechanisms of *meso*-hydroxylation by ferric hydroperoxide ($Fe^{III}OOH$) in the presence of H_3O^+ (additional data for this and the following mechanisms can be found in the Supporting Information deposited with this paper). Starting from the cluster $^2\mathbf{C}_R$, the *meso*-hydroxylation may follow two alternative mechanisms, one stepwise the other fully concerted. The stepwise mechanism starts with proton relay assisted-homolysis of the O−O bond, of the ferric hydroperoxide, to give an intermediate, $^2\mathbf{C}_I$, in which the OH• radical species is trapped by the electrostatic cage of the porphyrin (see inset, Figure 1). As shown recently,[7a] this complexation energy of the OH• radical species is substantial, and OH• cannot be considered as a free radical species. This interaction is also apparent from the structure of $^2\mathbf{C}_I$, which shows that the porphine ring is buckled in the direction of the OH• radical species. Moreover, the so trapped OH• is oriented over the *meso* carbon and ready for attack. In the second step, the OH• radical attacks the *meso* position of porphine to give the hydroxylated product. Note that the barrier for the second step is small as would be expected from addition of OH• to a double bond. As seen later, these mechanistic features are fixtures of the stepwise mechanism.

In the alternative mechanism, everything happens in concert; the proton moves from the H_3O^+ moiety to $Fe^{III}OOH$ complex, and concomitantly the O−O bond breaks, and the hydroxyl group is transferred to the *meso*-position. This is the concerted reaction, akin to the electrophilic mechanism proposed by Ortiz de Montellano et al.[1a,b,3] and Davydov et al.[5b] Comparing the two energy profiles, it is apparent that the stepwise mechanism has a lower barrier than the concerted one by 7.5/13.9 kcal/mol (on the energy/ZPE corrected energy scales). The same difference is obtained at the free energy scale (13.5 kcal/mol, see Supporting Information).

The structures of the transition states, $^2TS_{OOC}$ and $^2TS_{OO}$, in Figure 1 project the differences between the stepwise and the concerted mechanisms. It is seen that the higher activation

(16) de Visser, S. P.; Ogliaro, F.; Sharma, P. K.; Shaik, S. *J. Am. Chem. Soc.* **2002**, *124*, 11809.

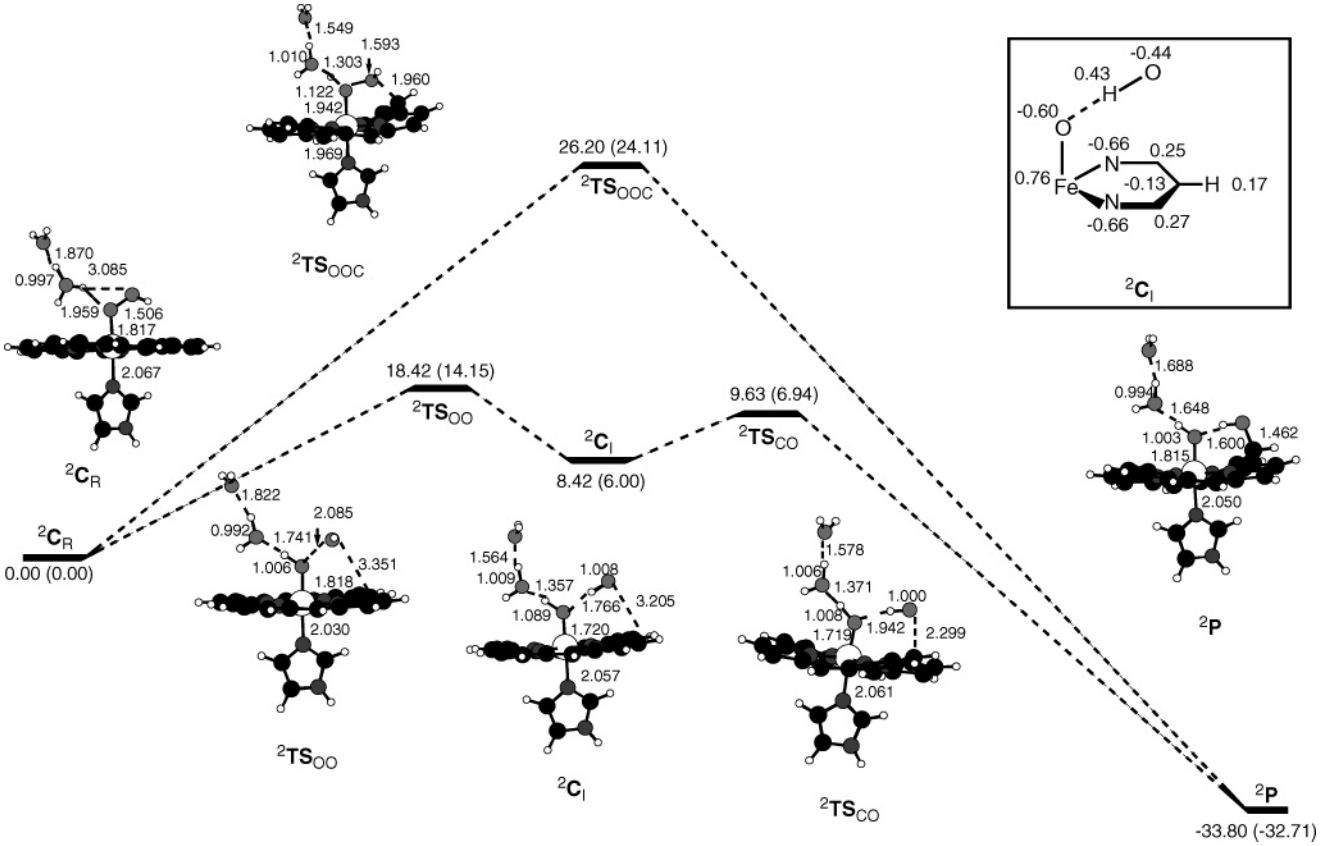

Figure 2. Concerted and stepwise energy profiles for hydroxylation of the *meso* carbon of porphine by the active species of heme oxygenase model with the $H_3O^+(H_2O)$ cluster. The energies are reported, relative to $^2\mathbf{C}_R$, and the values inside the parentheses include zero-point energy corrections. The drawing in the box shows the Coulombic cage trapping of the OH• radical species in the stepwise mechanism.

barrier for the concerted process is associated with further elongation of the Fe- - -O bond and the awkward O- - -C bonding (due to the rather acute OOC angle), as well as a more significant folding of the porphyrin ring, compared with the stepwise process. It should also be noted that the *meso* carbon in $^2TS_{OOC}$ is not undergoing simple pyramidalization distortion; rather, the entire C−C_{meso}−C moiety folds up like the lid of an envelope. To ascertain that this is not some artifact, we reoptimized the TS, now starting from a structure where the C−H_{meso} moiety is already pyramidalized. This reoptimization simply restored the original $^2TS_{OOC}$ structure. The same fold-type, but to a lesser extent, exists in $^2TS_{OO}$. This is true also for the rest of the transition states in the following discussion.

Figure 2 shows the same two mechanisms using the H_3O^+-(H_2O) cluster for protonation. Thus, starting from the cluster $^2\mathbf{C}_R$ the water cluster relays a proton to the proximal oxygen of the ferric hydroperoxide complex, in a Grotthuss-type fashion for both mechanisms.[9] The reaction profiles for the two mechanisms show once again that the stepwise homolytic process has a lower barrier by 7.8/10.0/13.4 kcal/mol (at the energy/energy + ZPE/ free energy scales). The TS structures indicate that, as in Figure 1, here too the reason is the loss of Fe−O bonding, an awkward O−C bonding in the concerted TS, and the acute porphine deformation, in comparison with $^2TS_{OO}$. As before, here too the deformation that exists in both transition states around the C−H_{meso} moiety is more buckling than pyramidalization.

Figure 3 shows the situation for the reaction catalyzed by the $H_3O^+(H_2O)_2$ cluster. The pattern repeats itself; the stepwise mechanism has a smaller barrier by as much as 11.9/13.6/18.8 kcal/mol at the energy/energy+ZPE/ free energy scales (see Supporting Information) compared with the concerted mechanism. As we noted above, the superiority of the stepwise mechanism is related to the intrinsically smaller deformation of the moieties that participate in the bond reorganization. It seems therefore, that *the energy advantage of the stepwise mechanism persists regardless of the number of water molecules in the cluster*.

To further ascertain that this trend is unaffected by the nature of the coordinating acid we used NH_4^+ instead of H_3O^+ and recalculated the two mechanisms. Figure 4 shows the same two mechanisms using the $NH_4^+(H_2O)_2$ cluster. As in all previous cases, here too the stepwise homolytic process has a lower barrier, now by 14.2/16.5 kcal mol^{-1} (energy/energy + ZPE). The TS structures exhibit features similar to the ones discussed above for the $H_3O^+(H_2O)_2$ clusters, and once again the deformation around the C−H_{meso} moiety is more buckling type than pyramidalization.

We performed a few more tests on the relative energies of the two transition states: the effect of polarity and the effect of the imidazole conformation relative to the FeOOH moiety. Table 1 collects these relative energies, including the previous results using bare ferric hydroperoxide,[7a] and protonated ferric hydrogen peroxide[7a] complexes. The results show that under all computational "experiments" the lowest energy transition state is the one for the stepwise mechanism, irrespective of the coordinating acid or the actual protonation state of the FeOOH moiety, or still of the conformation of the imidazole relative to the plane of the FeOOH moiety. Furthermore, introducing polarity effects, by use of a dielectric medium, either does not change or

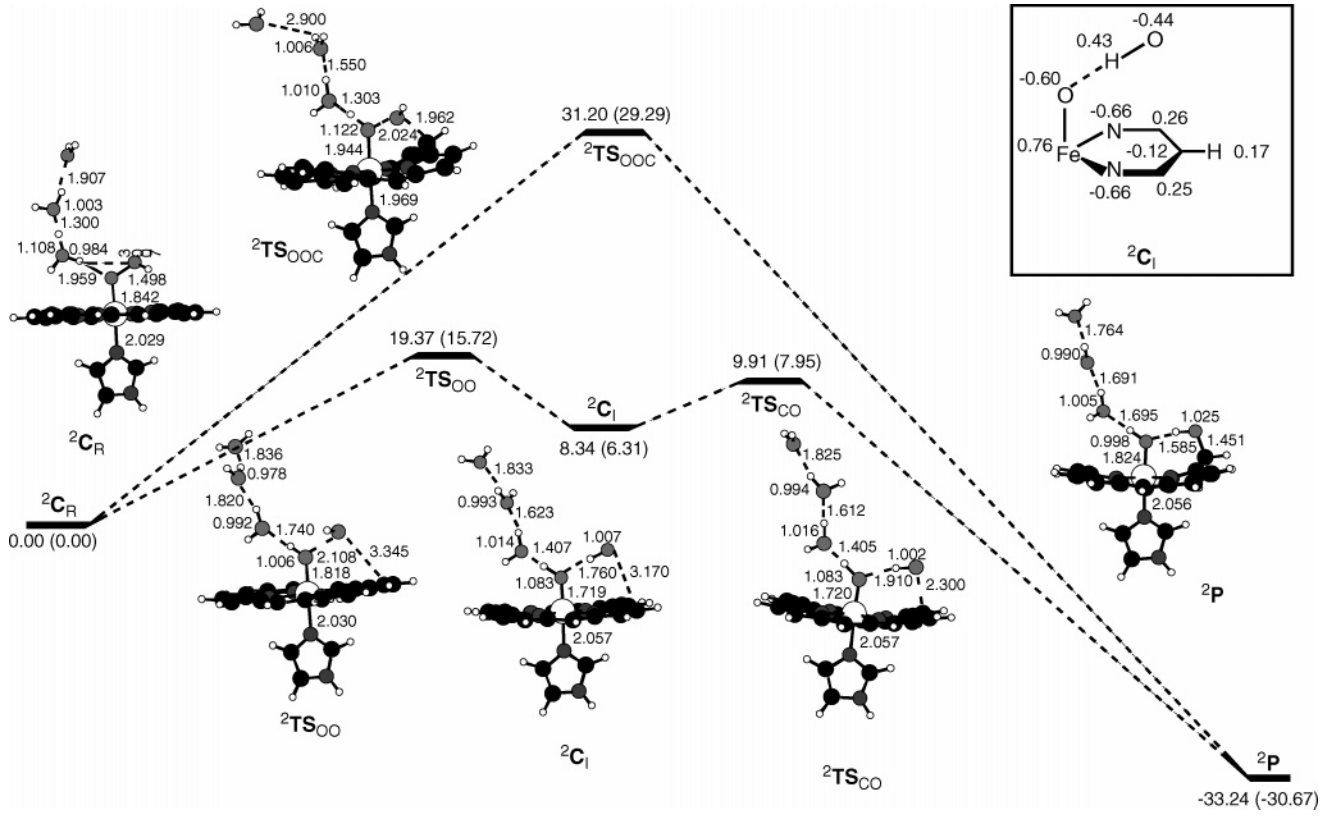

Figure 3. Concerted and stepwise energy profiles for hydroxylation of the *meso* carbon of porphine by the active species of heme oxygenase model with the $H_3O^+(H_2O)_2$ cluster. The energies are reported, relative to $^2\mathbf{C}_R$, and the values inside the parentheses include zero-point energy corrections. The drawing in the box shows the Coulombic cage trapping of the OH• radical species in the stepwise mechanism.

Table 1. Energy Destabilization[a] of the Transition State for the Concerted Mechanism ($^2TS_{ooc}$) Compared with the Stepwise ($^2TS_{oo}$) One

	$E(^2TS_{ooc}) - E(^2TS_{oo})$			
protonating species	with fixed[d] $R(O_a\cdots O_{last})$	without fixed $R(O_a\cdots O_{last})$	with ImH[e] perpendicular to FeOOH	$\epsilon = 5.7$[f]
H_3O^+	7.53	7.49	19.77	9.87
$H_3O^+(H_2O)$	7.77	7.67	12.85	11.95
$H_3O^+(H_2O)_2$	11.85	11.73	15.54	11.85
$H_4N^+(H_2O)_2$[b]	–	16.45	–	15.60
none[c]	–	24.9	–	–
(H^+)[c]	–	7.78	–	–

[a] In kcal/mol without ZPE correction. [b] Here dihedrals $N-O_2-O_a-O_b$ and $O_1-O_a-Fe-N_{por}$ are fixed. [c] From ref 7a. For the case of (H^+), the reaction starts from $Fe(H_2O_2)^+$. [d] O_{last} is the oxygen of the acid, H_3O^+, is Scheme 2. [e] Imidazole was rotated by 90° and the TSs were reoptimized. [f] The transition state structures in a dielectric medium with dielectric constant, $\epsilon = 5.7$.

increases the preference of the homolytic transition state, $^2TS_{OO}$, over its concerted counterpart, $^2TS_{OOC}$. Finally, releasing the constraints on the O_a- - -O_{last} distance has no effect on the advantage of the homolytic mechanism. It appears therefore, that *the energy advantage of the stepwise mechanism is significant and is indifferent* to the number of water molecules, to the nature or presence of an acid catalyst, at least in the representative sample we used to calculate these mechanisms here and previously.[7a] The sample of results involves a significant acidity scale, which covers the acidity of a neutral acid like Asp_{140}. Therefore, our model strongly suggests that the same mechanistic conclusion will persist inside the protein pocket.

What remains, therefore, is to look at the calculated kinetic isotope effects and judge whether they can indeed serve as intrinsic mechanistic probes of the heme species of HO. Table 2 collects all the solvent kinetic isotope effects (SKIEs) calculated for the two mechanisms. The datum in the last column is the experimental result that was measured at 215 K (estimated experimental value at 298 K = 1.8). To be consistent with the latter results we report the SKIEs for two temperatures, 215 and 298 K. Inspection of the data for the stepwise mechanism shows that the SKIE is consistently larger than unity. The best fit to the experimental datum is for the $H_3O^+(H_2O)_2$ cluster. The weaker acid $NH_4^+(H_2O)_2$ leads to overly large values for both mechanisms, and this indicates that the acidic center may well involve a water cluster coordinated to a carboxylic acid[2f−h,5b] rather than to a nitrogen acid. Interestingly, none of the results for the concerted mechanism fit the experimental datum as well as the fit of the stepwise mechanism with the $H_3O^+(H_2O)_2$ cluster. It follows, therefore, that the stepwise homolytic mechanism is energetically favorable and exhibiting a good match with experimental SKIE datum.[5b]

Table 2 also shows in the entries labeled as 5, SKIE values for the stepwise mechanism that involves an initial protonation of the ferric hydroperoxide to yield the ferric hydrogen peroxide complex, $Fe(H_2O_2)^+$, which then undergoes bond homolysis and OH• radical attack on the *meso* position, as reported in our previous study.[7a] For this mechanism too, the SKIE values do not match experiment and are significantly smaller than the experimental datum. The barriers for these stepwise mechanisms, nascent from $Fe(H_2O_2)^+$, are similar[7a] to those for the stepwise mechanisms in Figures 1−3. It is encouraging to find that an

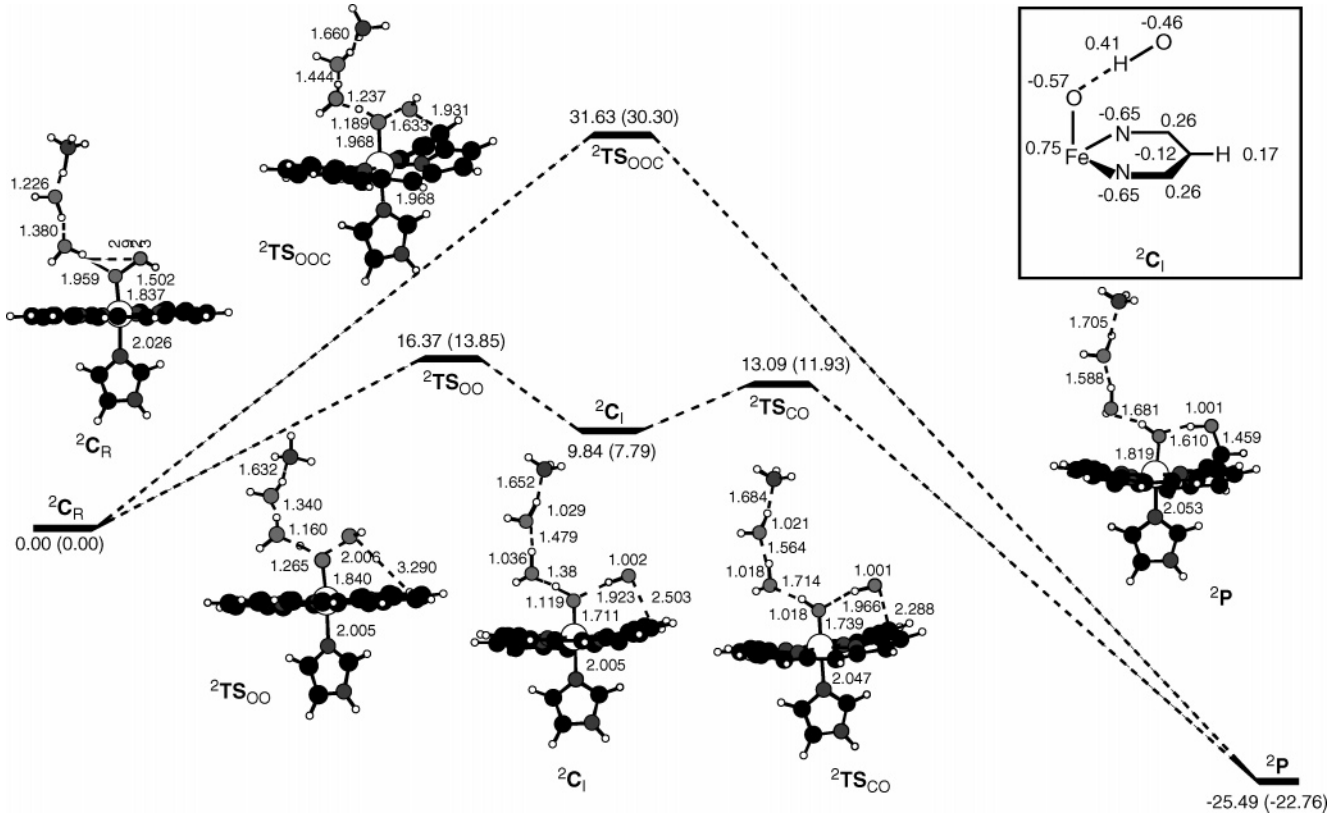

Figure 4. Concerted and stepwise energy profiles for hydroxylation of the *meso* carbon of porphine by the active species of heme oxygenase model with the $H_4N^+(H_2O)_2$ cluster. The energies are reported, relative to $^2\mathbf{C}_R$, and the values inside the parentheses include zero-point energy corrections. The drawing in the box shows the Coulombic cage trapping of the OH• radical species in the stepwise mechanism.

Table 2. Solvent Kinetic Isotope Effects (SKIEs) for the Mechanisms Depicted in Figures 1−4, and for the Mechanism that Starts from the Initially Protonated, $Fe(H_2O_2)^+$ Species

		SKIE values				
		stepwise mechanism		concerted mechanism		experimental datum[b]
entry	protonating species	$T = 215$ K[a]	$T = 298$ K[a]	$T = 215$ K[a]	$T = 298$ K[a]	215 K(298 K)
1	H_3O^+/D_3O^+	2.57 (2.58)	2.30 (2.30)	3.06 (3.08)	2.45 (2.45)	2.3 (1.8)
2	$H_3O^+(H_2O)/D_3O^+(D_2O)$	1.31 (1.32)	1.25 (1.26)	1.36 (1.54)	1.16 (1.16)	
3	$H_3O^+(H_2O)_2/ D_3O^+(D_2O)_2$	2.23 (2.24)	1.91 (1.92)	4.04 (4.05)	2.91 (2.91)	
4	$H_4N^+(H_2O)_2/H_3ND^+(D_2O)_2$	4.69	3.45	3.72	2.93	
5	$Fe(H_2O_2)^+$, $1H_2O$[c]	1.74	1.62	1.32	1.47	
	$Fe(H_2O_2)^+$, $2H_2O$[c]	1.28	1.24	1.42	1.36	
	$Fe(H_2O_2)^+$, $3H_2O$[c]	1.46	1.36	1.24	1.22	

[a] In parentheses are values corrected for tunneling, using the Wigner correction (as in ref 16). [b] From ref 5b. [c] These SKIE refer to the mechanism in ref 7a, where the FeOOH species is initially protonated to $Fe(H_2O_2)^+$.

initial protonation of the FeOOH species is excluded by the computed and experimental[5b] SKIE values. Otherwise, it would have been exceedingly difficult to understand why the protonation should occur on the proximal position, but not on the distal oxygen, where it would have led to the formation of the high-valent oxo−iron species, after elimination of a water molecule (a peroxidase-type activity of HO). Indeed, the structural data,[2a,e,f] shows that there is no specific acid close enough to the FeOOH moiety to partake directly in a protonation reaction, but there exists a hydrogen-bonding network that connects to the distal side[2c−h,8] of the heme. Thus, *a mechanism where the proton is relayed regiospecifically, via a structured water chain, to the proximal oxygen of FeOOH species while the O−O bond is undergoing homolysis emerges as a logical solution to this dilemma too*. In this respect, our results are in accord with the experimentally deduced mechanism[5b] that protonation is synchronous with and does not occur before the O−O bond activation in the ferric hydroperoxide species.

It is instructive at this point to inspect, with some more details, the best fitting transition state, i.e., the bond homolysis transition state for the case of the $H_3O^+(H_2O)_2$ cluster, and compare its structure and electronic features to the transition of the corresponding concerted mechanism. This is done in Figure 5, which displays the two species alongside each other. The greater deformation of the concerted $^2TS_{OOC}$ species is apparent; however, as noted above, the deformation does not really pyramidalize the $(C_2N_2)CH_{meso}$ moiety of the porphyrin. In fact, the sum of the three angles around the *meso* carbon is almost 360° for both transition states, and this is true for all others in this study (Figures 1−4), irrespective of the number of water molecules. Thus, intrinsically the heme does not reveal pyramidalization of the *meso* position in either TS species, but rather

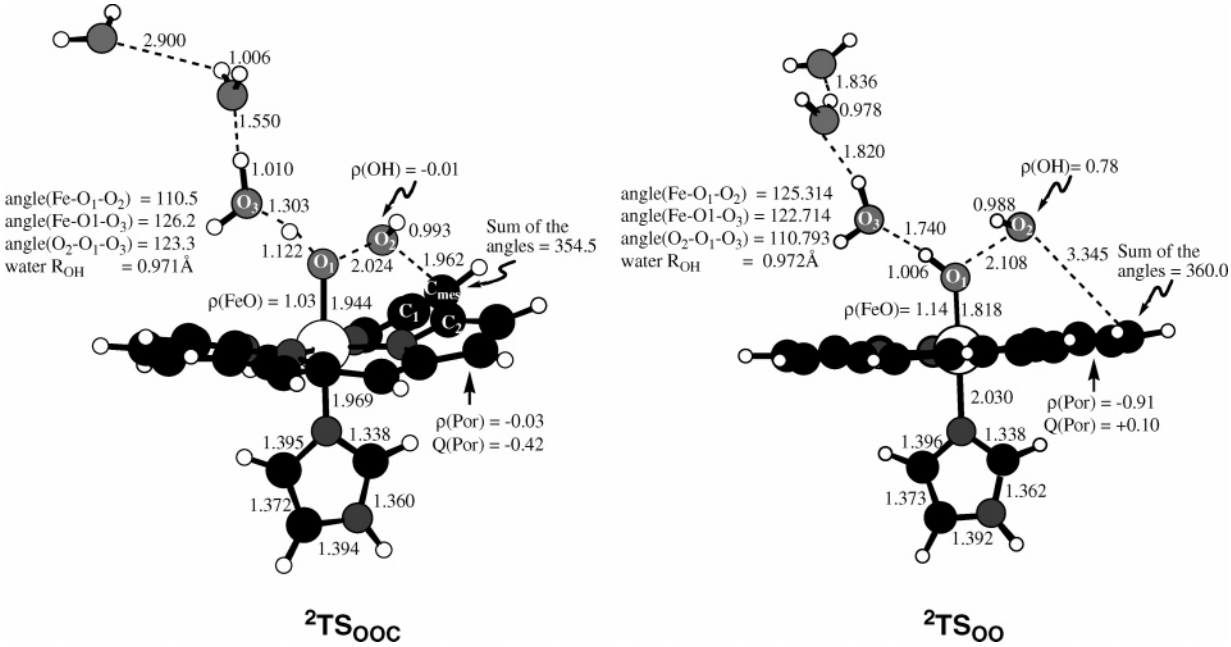

Figure 5. Key geometric features of $^2TS_{OOC}$ and $^2TS_{OO}$ for the case of the $H_3O^+(H_2O)_2$ cluster. Some spin density values, ρ, and charges, Q, are indicated near the respective groups.

Table 3. α-Deuterium Secondary Kinetic Isotope Effects (*sec*-KIEs) Values Calculated for the Mechanisms in Figures 1−4

		sec-KIEs[a] values				
		stepwise mechanism		concerted mechanism		experimental datum[b]
entry	protonated species	$T = 215$ K[a]	$T = 298$ K[a]	$T = 215$ K[a]	$T = 298$ K[a]	215 K(298 K)
1	H_3O^+	0.98 (0.98)	0.98 (0.98)	0.98 (0.98)	0.96 (0.96)	0.7 (0.8)
2	$H_3O^+(H_2O)$	0.98 (0.98)	0.98 (0.98)	1.00 (1.00)	1.00 (1.00)	
3	$H_3O^+(H_2O)_2$	0.98 (0.95)	0.98 (0.98)	0.99 (0.99)	1.00 (1.00)	
4	$H_4N^+(H_2O)_2$	0.98 (0.98)	0.98 (0.98)	0.99 (0.99)	1.00 (1.00)	

[a] In parentheses are values corrected for tunneling, using the Wigner correction. [b] From ref 5b.

some buckling that is greater in the concerted path. In addition, in both $^2TS_{OOC}$ and $^2TS_{OO}$, the environment of the CH_{meso} becomes more crowded, relative to that of the reactant state, due to the coordination of OH to the *meso*-CH moiety and its Coulombic caging by the porphyrin (see insets, Figures 1−4).

A most interesting change occurs in the electronic structure during the two mechanisms. The reactant cluster, ^2C_R, is a doublet state, with virtually all the spin density residing on the iron[7a] (see Supporting Information). In the concerted mechanism, the $^2TS_{OOC}$ species conserves this electronic structure; all the spin resides on the iron with negligible development on the porphyrin and the transferred OH moiety (see Figure 5). By contrast, in the $^2TS_{OO}$ species of the stepwise mechanism there is spin density development, close to unity, on the transferred OH group as well as on the porphyrin. Thus, the porphyrin attains in the bond homolysis transition state a radical cationic situation, as can also be deduced from the fact that the porphyrin charge (Q(Por)) is positive in contrast to the negative charge in the concerted $^2TS_{OOC}$ species (Figure 5). The negative charge and lack of spin density on the porphyrin typify also the reactant cluster, $^2\mathbf{C}_R$, (Q(Por) = −0.60, see Supporting Information). In the intermediate, $^2\mathbf{C}_I$, the porphyrin is almost neutral and (Q(Por) = −0.09), and the spin density on iron is close to two, corresponding to an Fe^{IV} center. As such, the stepwise mechanism starts with a $PorFe^{III}$ situation, proceeds to the $^2TS_{OO}$ species with a unique electronic structure that resembles a $Por^{+\bullet}Fe^{III}OH$- - -HO• species, and continues to the intermediate, $^2\mathbf{C}_I$, which is a $PorFe^{IV}OH$- - -HO• species. It should be noted that the same applies, with small changes, to all other $^2TS_{OO}$ species, irrespective of the water cluster size, with the exception of the $H_4N^+(H_2O)_2$ cluster, where the corresponding $^2TS_{OO}$ species is already of the $PorFe^{IV}OH$- - -HO• variety as is the corresponding intermediate (both having almost neutral porphyrin moieties; see Supporting Information). The diminished negative charge on the porphyrin in the $^2TS_{OO}$ species will further aid to clump the OH group by Coulombic interactions, and this may certainly contribute to the stability of the $^2TS_{OO}$ species compared with that of the respective $^2TS_{OOC}$ species in the concerted mechanism.

Having clarified the unique structural and electronic features of the $^2TS_{OO}$ species, we can turn to inspect the *intrinsic values* of the α-deuterium secondary kinetic isotope effects (*sec*-KIEs) for the two mechanisms. Table 3 displays the *sec*-KIE values for the attack on the *meso* position ($C-H_{meso}/C-D_{meso}$). The values for the stepwise process are smaller than unity, the smallest value arises for the case of the $H_3O^+(H_2O)_2$ cluster where it reaches 0.95 with a Wigner tunneling correction. Interestingly, the values for the concerted mechanism are all closer to unity compared with those of the respective stepwise mechanisms. The nonsignificant *sec*-KIEs of the concerted mechanism seems somewhat surprising, considering the acute deformation of the porphine ring near the *meso* site, in the structures of the concerted $^2TS_{OOC}$ species in Figures 1−4. However, as we noted above, the structural deformation in both

Table 4. Secondary Kinetic Isotope Effect (*sec*-KIEs) of the Double Bond Activation of Propene with a Model of the High-Valent Oxo−Iron Species of P450

	sec-KIE[a]	
isotopic species	HS[b]-mechanism	LS[b]-mechanism
$CH_3CH{=}CH_2/CH_3CH{=}CHD$	0.87	0.87
$CH_3CH{=}CH_2/CH_3CH{=}CD_2$	0.75	0.75

[a] $T = 215$ K. [b] HS corresponds to the quartet high spin mechanism and LS to low spin one. See ref 16 for mechanistic details.

$^2TS_{OOC}$ and $^2TS_{OO}$ is not a pyramidalization of the $(N_2C_2)C-H_{meso}$ moiety of the porphyrin but rather a folding mode that leaves the moiety virtually planar. We recall that reoptimization of the $^2TS_{OOC}$ structure, starting from a geometry where the $(N_2C_2)C-H_{meso}$ moiety is initially pyramidalized, *restored the original unpyramidalized structure*. Hence, if this intrinsic structural feature is also correct in the enzyme pocket, then *sec*-KIE is not a probe that can distinguish the two mechanisms; furthermore, the classical interpretation of the observed *sec*-KIE as a probe of the degree of rehybridization in the transition state ought to be reconsidered. At least in the cases of $^2TS_{OOC}$ and $^2TS_{OO}$ studied here, the inverse calculated value may reflect some crowding near the $(N_2C_2)C-H_{meso}$ moiety, as well as stiffening of the $C-H_{meso}$ movements due to the Coulombic caging of the OH group by the $(N_2C_2)C-H_{meso}$ moiety (see insets, Figures 1−4). The electronic structure of $^2TS_{OO}$ suggests that the decreased electronic charge in the porphyrin will increase the interaction with the negatively charged oxygen of the OH group compared with the concerted transition state. These Coulombic interactions may stiffen the out-of-plane bending and stretching vibrations of $C_{meso}-H$ and cause the slightly more inverse *sec*-KIEs for the stepwise homolytic mechanism.

Still, however, the calculated *sec*-KIE values are substantially less inversed compared with the experimental datum (0.7, Table 3). One might have thought that the quantitative difference may reflect inaccuracies of the DFT method. To ascertain that the B3LYP/LACVP calculations do not systematically underestimate the *sec*-KIEs, we investigated this quantity for a model system that involves attack of the high-valent iron−oxo compound I species on the CH_2 group of propene during double bond epoxidation.[16] These values are collected in Table 4, and are seen to be inverse and in the range of other experimental data for a single hydrogen (deuterium), C−H(D).[6a] It follows, therefore, that the level of theory is able to pick up the subtle effects required to reproduce *sec*-KIE values due to pyramidalization of the $C(sp^2)-H$ moiety in the TS. What could then be the cause of the quantitative disparity in the case of the model HO calculations in Table 3?

A very inverse *sec*-KIE value may reflect stiffening of the out-of-plane bending and/or stretching $C-H_{meso}$ vibrations in the transition state, either due to the electric field of the protein or to steric constraints inside the pocket.[17] Indeed, computational studies, over the years, have shown that there is no simple correlation between the value of the *sec*-KIE and the geometry of the transition states. The value appears to be influenced by out-of-plane C−H bending,[6a] by C−H stretching,[17b−e] and by tightness/looseness of the carbon undergoing bonding changes[17f] as well by polarity effects on the movements of the C−H bond.[17a] For example, a recent QM/MM study[17a] cautions against the interpretation of *sec*-KIE as a measure of transition-state structure along the classical guidelines and shows that the increased inverse value of the *sec*-KIE in an enzymatic environment arises from the stiffening of the out-of-plane C−H vibration in the transition state due to more favorable electrostatic interactions with the protein environment. A similar effect might happen in the case of the homolytic mechanism of HO, especially since *the porphyrin moiety undergoes an inversion of its charge from negative in the reactants to positive in $^2TS_{OO}$* (see Figure 5 above). Additionally, upon folding deformation, slight as it may be in $^2TS_{OO}$, the $C-H_{meso}$ moiety will encounter increased steric/electrostatic interactions with Leu_{147} (which is initially only 3.71 Å from H_{meso}); this may then stiffen the C−H motion in the transition states and contribute to an inverse isotope effect.[18] However, this cannot be properly addressed in a QM calculation and is beyond the scope of the present study.

Thus, taking the results in Table 3 at their face values, it is clear that the concerted mechanism does not have an intrinsic *sec*-KIE value that can support the classical interpretation of a rehybridization effect.[6a] The sense of the computed effect (<1) is provided by the stepwise homolytic mechanism catalyzed by the $H_3O^+(H_2O)_2$ cluster even though there is no apparent rehybridization in the *meso* carbon. Accordingly, the strong deviation from the experimental value indicates that intrinsically the rehybridization effect at the *meso* site is too small to account for the observed *sec*-KIE. We tentatively propose that effects other than the classical bonding changes at the *meso* carbon must be responsible for the experimental observation.[5b,18]

The homolytic mechanism is not new. It was suggested for HO itself by Rivera et al.[19] It is known for related systems, which involve FeOOH or FeOOR (R = alkyl, etc.) moieties.[20] In fact, it was considered originally by Ortiz de Montellano and co-workers[1a,b,3] as a potential mechanistic alternative but was discarded since such a mechanism would have produced nonselective OH• radical species, whereas the HO enzyme leads to a regiospecific *meso*-hydroxylation. However, as the present theoretical study shows, *the OH• radical species is bound*. The Coulombic cage of the porphyrin binds the radical that hangs, in the $^2\mathbf{C}_I$ intermediate, just on top of the *meso* position, ready for a regiospecific attack. Once bound, the OH radical will hydroxylate the corresponding *meso* position. The regiospecificity for the α-position may be partially driven by the facts that, in the crystal structure,[2a,g] the $Gly_{135,139}$ residues (in human HO) block all other *meso* directions except for α, while at the

(17) (a) Ruggiero, G. D.; Williams, I. H. *J. Am. Chem. Soc.* **2004**, *126*, 8634. (b) Zhao, X. G.; Tucker, S. C.; Truhlar, D. G. *J. Am. Chem. Soc.* **1991**, *113*, 826; Viggiano, A. A.; Paschkewitz, J. S.; Morris, R. A.; Paulso, J. F.; Gonzalz-lafon, A.; Truhlar, D. G. *J. Am. Chem. Soc.* **1991**, *113*, 9404. (c) Wolfe, S.; Kim, C.-K. *J. Am. Chem. Soc.* **1991**, *113*, 8056. (d) Boyd, R. J.; Kim, C.-K.; Shi, Z.; Weinberg, N.; Wolfe, S. *J. Am. Chem. Soc.* **1993**, *115*, 10147. (e) Glad, S. S.; Jensen, F. *J. Am. Chem. Soc.* **1994**, *116*, 9302. (f) Poirier, R. A.; Wange, Y.; Westaway, K. C. *J. Am. Chem. Soc.* **1994**, *116*, 2526.

(18) Viewing the HO structure of the oxy complex[2g] (PDB 1V8X), one may conclude that if the deformation in the TS is the folding deformation as in $^2TS_{OO}$ then the $C-H_{meso}$ moiety will get closer to the protein residue Leu_{147}, which initially has a 3.71 Å distance to the H_{meso}. This may induce stiffening of the $C-H_{meso}$ motion in the transition state.

(19) Rivera, M.; Caignan, G. A.; Astashkin, A. C.; Raitsimring, A. M.; Shokhireva, T. Kh.; Walker, F. A. *J. Am. Chem. Soc.* **2002**, *124*, 6077.

(20) For a small sample of available papers, see: (a) Nam, W.; Kim, M. H.; Moon, S. K.; Kim, C. *J. Am. Chem. Soc.* **2000**, *122*, 10805. (b) Robert, A.; Coppel, Y.; Meunier, R. *Chem. Commun.* **2002**, 414. (c) Robert, A.; Coppel, Y.; Meunier, R. *Inorg. Chim. Acta* **2002**, *339*, 488. (d) Allentoff, A. J.; Bolton, J. L.; Wilks, A.; Thompson, J. A.; Ortiz de Montellano, P. R. *J. Am. Chem. Soc.* **1992**, *114*, 9744. (e) Kaizer, J.; Costas, M.; Que, L., Jr. *Angew. Chem., Int.* **2003**, *42*, 3671.

Table 5. Some Kinetic Isotope Effect Probes in the Stepwise and Concerted Mechanism[a]

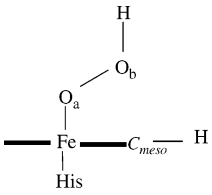

KIE Probe	stepwise mechanism $T = 215$ K (298 K)	concerted mechanism $T = 215$ K (298 K)
$C_{12/14}$	1.01 (1.01)	1.06 (1.07)
$O^{(a)}{}_{16/18}$	1.02 (1.01)	1.04 (0.98)
$O^{(b)}{}_{16/18}$	1.13 (1.10)	1.06 (1.06)
$O^{(a+b)}{}_{16/18}$	1.15 (1.11)	1.10 (1.04)
$O^{(a+b)}{}_{16/18}$ & $C_{14/12}$	1.14 (1.10)	1.04 (0.99)
$O^{(b)}{}_{16/18}$ & $C_{14/12}$	1.12 (1.09)	1.00 (1.01)
$O^{(b)}{}_{18/16}$ & $C_{14/12}$	0.90 (0.92)	1.00 (0.99)

[a] All calculations refer to the TSs with the $H_3O^+(H_2O)_2$ cluster.

same time the α-position is the only *meso* direction that appears to be relatively free of steric hindrance to fold up, as found here, and assist the hydroxylation. In fact, since the rate-determining step is the O−O bond homolysis and since the OH• radical is strongly bound, the stepwise mechanism is effectively concerted, and *in this sense, our proposed mechanism provides general support for the mechanism deduced by Davydov et al. from experiment.*[5b] Thus, while experimental *sec*-KIE data is interpreted to originate from a fully concerted mechanism, the support for this interpretation rests on an older modeling of this probe.[6a,b] Modern considerations of *sec*-KIE,[17] show that the classical interpretation that the effect reflects the $sp^2 \rightarrow sp^3$ hybridization in the TS will often, albeit not always, be misleading. Unfortunately, a reliable and definitive treatment of *sec*-KIE within the enzyme pocket is still beyond our present capability. Nevertheless, the theoretical results in this contribution indicate that a different interpretation, based on a homolytic O−O cleavage mechanism, is possible; it accounts for the fast rate of the heme degradation reaction and the experimental SKIE probe, and suggests that an alternative solution for the inverse *sec*-KIE is also possible.[17,18]

To suggest further experiments, which may distinguish between the homolytic and concerted mechanisms, we collected in Table 5 two more KIE probes. One probe is the $CKIE_{12/14}$ that measures the isotope effect due to changes of the isotopic identity of the *meso*-carbon. It is seen that the $CKIE_{12/14}$ value that is significantly larger for the concerted mechanism may serve as an additional probe of the bonding changes in the *meso* carbon in the transition states. The second probe is the $OKIE_{16/18}{}^{(a+b)}$ that measures the isotope effect due to O_a-O_b bond cleavage in the transition states. It is seen that this quantity is larger for the stepwise homolytic mechanism. A combination KIE may be the best probe for distinguishing the two mechanisms; for example, the combination $OKIE_{16/18}{}^{(a+b)}CKIE_{14/12}$ is 1.10 (298 K) for the stepwise mechanism and 0.99 (298 K) for the concerted mechanism.

In addition to these KIE probes, the homolytic mechanism with hydroxylation from a "bound hydroxyl radical"[21] suggests that, under some mutations, a small fraction of the bound HO• radical could be pulled out from the caging of the porphyrin and lead to the formation of compound I of HO, to a mixed HO/peroxidase activity, and to some oxidation of the protein residue.

Concluding Remarks

The density functional calculations described in this report address the mechanism of heme degradation by the enzyme heme oxygenase (HO),[3,5b] using model systems.[7a] The present paper studies the stepwise and concerted mechanisms (using $H_3O^+(H_2O)_n$, $n = 0-2$, and $H_4N^+(H_2O)_2$ as proton relay systems) and provides barriers and kinetic isotope effects. It shows that a stepwise mechanism that involves proton relay and O−O homolysis, in the rate-determining step, has a lower barrier (≥10 kcal/mol) than the corresponding fully concerted mechanism. The conclusion that the proton relay occurs with O−O bond homolysis in a stepwise but quasi-concerted manner from a "bound OH radical"[21] (since the second barrier is small) appears consistently in all the calculations (see Table 1), here and before,[7a] and covers a range of acid strengths sufficiently large to suggest that the conclusion is not specific only to the model system.

A good fit of the calculated SKIE to the experimental data[5b] is obtained for the cluster $H_3O^+(H_2O)_2$. The calculations show that intrinsically the values of the *sec*-KIE for either the homolytic (0.95) or the concerted mechanism (0.99) are slightly inversed, but quantitatively far off, from the experimental value (0.7). The fact that the concerted mechanism simply does not match the experimental datum, suggests that the experimental datum[5b] for HO probably probes effects that are not intrinsic to the active species itself. Indeed, considering all the possible factors that go into a particular *sec*-KIE value,[17] the classical interpretation based only on rehybridization on the site of attack may not apply to this case; alternative explanations may exist,[18] which are based on the stiffening of the $C-H_{meso}$ movement in the transition state. This and the suggestions of additional mechanistic probes, which can distinguish between the two mechanisms, demonstrate that theory can promote a useful dialogue with experiment.

Acknowledgment. The research was supported by an ISF grant to S.S. Helpful discussions with T.L. Poulos and P.R. Ortiz de Montellano are acknowledged.

Supporting Information Available: Seventeen tables, and 11 figures with structures and profiles. This material is available free of charge via the Internet at http://pubs.acs.org.

JA0446956

(21) For a recent cover story of "bound OH radical" and its potentially great oxidative power, see: Wilson, B. *Chem. Eng. News* **2005**, *January 31st Issue, 39.*